







Another new karst-dwelling rock gecko in the *Cnemaspis siamensis* group (Reptilia, Gekkonidae) from Kanchanaburi Province, western Thailand

Attapol Rujirawan^{1,2}, Akrachai Aksornneam¹, Siriporn Yodthong³, Parinya Pawangkhanant⁴,
Bryan L. Stuart⁵, Anchalee Aowphol^{1,2}

¹ Animal Systematics and Ecology Speciality Research Unit, Department of Zoology, Faculty of Science, Kasetsart University, Bangkok 10900, Thailand

² Biodiversity Center Kasetsart University (BDCKU), Bangkok 10900, Thailand

³ Department of Biological Science, Faculty of Science, Ubon Ratchathani University, Ubon Ratchathani 34190, Thailand

⁴ Rabbit in the Moon Foundation, Suan Phueng, Ratchaburi 70180, Thailand

⁵ North Carolina Museum of Natural Sciences, 11 West Jones Street, Raleigh, North Carolina 27601, USA

Corresponding author: Anchalee Aowphol (fsciac@ku.ac.th)



Academic editor: Luis Ceríaco

Received: 3 October 2024

Accepted: 17 December 2024

Published: 6 February 2025

ZooBank: <https://zoobank.org/BA9E743F-0D1A-4EEF-BFE6-150645326066>

Citation: Rujirawan A, Aksornneam A, Yodthong S, Pawangkhanant P, Stuart BL, Aowphol A (2025) Another new karst-dwelling rock gecko in the *Cnemaspis siamensis* group (Reptilia, Gekkonidae) from Kanchanaburi Province, western Thailand. ZooKeys 1226: 1–24. <https://doi.org/10.3897/zookeys.1226.138464>

Copyright: © Attapol Rujirawan et al.
This is an open access article distributed under terms of the Creative Commons Attribution License (Attribution 4.0 International – CC BY 4.0).

Abstract

A new species of the *Cnemaspis siamensis* group is described from Wang Khrachae District, Kanchanaburi Province, western Thailand based on morphological and molecular data. The new species, *Cnemaspis enneaporus* Rujirawan, Aksornneam & Aowphol, **sp. nov.**, is distinguished from other species in the *C. siamensis* group by having the combination of SVL 42.2 mm in adult male ($n = 1$), 43.7 mm in adult female ($n = 1$); eight supralabials; seven or eight infralabials; ventral scales smooth; nine continuous precloacal pores in male; 17 or 18 paravertebral tubercles linearly arranged; tubercles on lower flanks present; lateral caudal furrows present; no caudal tubercles in the lateral furrows; ventrolateral caudal tubercles present on original portion of tail; caudal tubercles not encircling tail; subcaudals smooth; no enlarged median subcaudal row; two postcloacal tubercles on each side of tail; no shield-like subtibial scales; subtibial scales smooth; no enlarged submetatarsal scales; 26–28 subdigital lamellae on the fourth toe; sexually dimorphic for dorsal and ventral colour pattern; prescapular marking absent; gular marking absent; and yellow colouration in life on all ventral surfaces of head, body and tail in adult male. Phylogenetically, the new species is recovered as the sister taxon to *C. huaseesom*, but the two species are separated by 8.3–9.4% uncorrected pairwise genetic divergences in the mitochondrial NADH dehydrogenase subunit 2 gene and flanking tRNAs.

Key words: *Cnemaspis enneaporus*, karst formations, molecular phylogenetics, morphology, Tenasserim Mountain Range

Introduction

The rock gecko genus *Cnemaspis* Strauch, 1887 is the second-most diverse gekkonid genus with 227 named species (Karunaratna et al. 2023; Uetz et al. 2024). *Cnemaspis sensu stricto* (= Southeast Asian *Cnemaspis*; sensu Grismer et al. 2014), hereafter *Cnemaspis*, contains at least 69 Sundaic and Indochinese

species that are distributed from southern Laos, Vietnam, Cambodia, and Thailand, and southwards through Thai-Malay peninsula, Sumatra, Java, and eastwards to Borneo (Grismer et al. 2010, 2014; Riyanto et al. 2019; Ampai et al. 2022; Nashriq et al. 2022; Rujirawan et al. 2022; Kurita et al. 2024). In Thailand, *Cnemaspis* comprises 22 named species from two major clades (the Northern Sunda and Pattani clades; sensu Grismer et al. 2014). For the Northern Sunda clade, Thai *Cnemaspis* have been assigned to three species groups (the *C. affinis*, *C. chanthaburiensis*, and *C. siamensis* groups) based on morphology and molecular phylogenies (Grismer et al. 2014; Wood et al. 2017; Ampai et al. 2019, 2020, 2022; Rujirawan et al. 2022). The *siamensis* group is the most diverse species group in Thailand, comprising 16 nominal species that are distributed along the Thai-Malay Peninsula from Kanchanaburi Province in western Thailand southwards through the Isthmus of Kra region in southern Thailand (mainland and adjacent islands) and Langkawi Island, Peninsular Malaysia (Grismer and Chan 2010; Ampai et al. 2022; Rujirawan et al. 2022). Recently, *C. auriventralis* Rujirawan, Yodthong, Ampai, Termprayoon, Aksornneam, Stuart & Aowphol, 2022 was described from Erawan National Park and is closely related to *C. huaseesom* Grismer, Sumontha, Cota, Grismer, Wood, Pauwels & Kunya, 2010 from Sai Yok National Park (Grismer et al. 2010; Rujirawan et al. 2022). Both species were described from Kanchanaburi Province, western Thailand (ca 25 km between their type localities) and from similar habitat and substrate (karst associated area), but differ in elevational zonation (upland in *C. auriventralis* and lowland in *C. huaseesom*) (Grismer et al. 2014; Rujirawan et al. 2022).

In November 2022, two specimens of *Cnemaspis* were collected from karst forest in Wang Khrachae Subdistrict, Sai Yok District, Kanchanaburi Province, western Thailand (Fig. 1). This population closely resembled *C. auriventralis* in colour pattern (all ventral surfaces of head, body and tail yellow in adult male) and microhabitat. Our morphological and molecular results reveal that the Wang Khrachae samples differ from *C. auriventralis* and other known species of the *C. siamensis* group. We herein described this population as a new species.

Materials and methods

Sampling

Cnemaspis specimens were collected from Wang Khrachae Subdistrict, Sai Yok District, Kanchanaburi Province, western Thailand in November 2022 (Fig. 1). Geographic coordinates and elevations were recorded using a Garmin GPSMAP 64s with WGS84 datum. Live animals and preserved specimens were photographed using a Nikon Z50 digital camera with an AF-S Micro Nikkor 60-mm f/2.8G ED lens and external flashes. Captured specimens were humanely euthanised using tricaine methanesulfonate (MS-222) (Simmons 2015). Liver tissues were immediately removed from euthanised individuals, preserved in 95% ethanol and stored at -20 °C for molecular analysis. Euthanised specimens were fixed in 10% formalin and later transferred to 70% ethanol for permanent storage. Specimens and tissues were deposited in the herpetological collection of the Zoological Museum, Kasetsart University, Thailand (**ZMKU**).

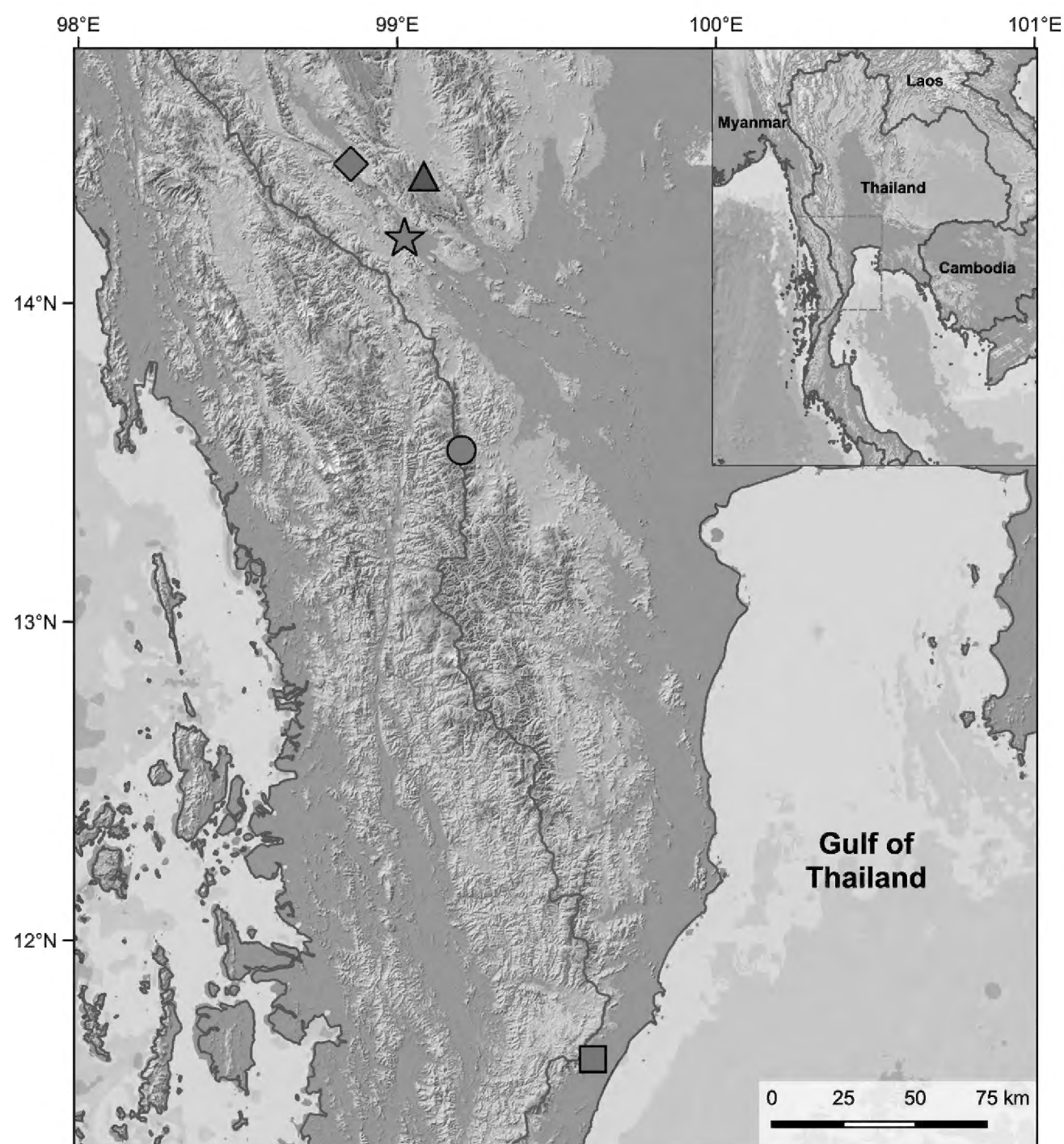


Figure 1. Map illustrating the type localities of *Cnemaspis enneaporus* sp. nov. (red star) at Wang Khrachae Subdistrict, Sai Yok District, Kanchanaburi Province, Thailand and its close relatives, *C. auriventralis* (green triangle), *C. huaseesom* (yellow diamond), *C. punctatonuchalis* (blue rectangle), and *C. selenolagus* (orange circle).

DNA extraction and PCR amplification

We extracted genomic DNA from liver tissue of two individuals of *Cnemaspis* from Wang Khrachae Subdistrict, Sai Yok District, Kanchanaburi Province (Fig. 1, Suppl. material 1) using the DNeasy Blood and Tissue Kit (Qiagen, Germany) according to the manufacturer's protocol. The mitochondrial NADH dehydrogenase subunit 2 gene (ND2) and its flanking tRNAs was amplified via a double-stranded polymerase chain reaction (PCR) using the light strand primer L4437b (5'-AAGCAGTTGGGCCCATACC-3'; Macey et al. 1997) and heavy strand primer H5934 (5' AGRGTGCCAATGTCTTTGTGRTT-3'; Macey et al. 1997). PCR reactions were executed in an Eppendorf Mastercycler gradient thermocycler under the following conditions: initial denaturation at 95 °C for 2 min, followed by a second denaturation at 95 °C for 35 s, annealing at 55 °C for 35 s, followed by a cycle extension at 72 °C for 35 s, for 33–40 cycles with a final extension at 72 °C for 10 min. PCR products were purified using a QIAquick PCR Purification Kit (Qiagen, Germany). PCR products were sequenced in both forward and reverse directions using the same amplifying primers at Bio Basic Asia Pacific PTe Ltd (Singapore) on an ABI 3730XL automatic sequencer.

(Applied Biosystems, CA, USA). Sequences were visually checked and edited in Geneious Prime 2021.0.3 (<https://www.geneious.com>). The protein-coding region of ND2 was translated to amino acids and checked to confirm the lack of premature stop codons. All new sequences were deposited in GenBank under accession numbers PQ659222–PQ659223 (Suppl. material 1).

Phylogenetic analyses

Additional homologous sequences of 80 individuals belonging to the *C. affinis* group, *C. boulengeri* group, *C. argus* group, *C. chanthaburiensis* group, *C. kumpoli* group (= Pattani clade in Grismer et al. 2014), *C. siamensis* group and outgroups were downloaded from GenBank. *Cyrtodactylus bokorensis* Murdoch, Grismer, Wood, Neang, Poyarkov, Tri, Nazarov, Aowphol, Pauwels, Nguyen & Grismer, 2019 and *Hemidactylus garnotii* Duméril & Bibron, 1836 were selected as outgroups to root the tree following Ampai et al. (2022) and Rujirawan et al. (2022). The two newly generated and downloaded *Cnemaspis* sequences were aligned using MAFFT v.7 online service (<https://mafft.cbrc.jp/alignment/server/index.html>; Katoh and Standley 2013). The aligned dataset was partitioned into four partitions consisting of 1st–3rd ND2 codon positions and tRNAs. Best-fit models of evolution for each partition were determined with ModelFinder (Kalyaana-moorthy et al. 2017) using the Bayesian information criterion (BIC). The best-fit evolutionary models were TPM2u+F+I+G4 for tRNAs and TVM+F+I+G4, TIM3+F+I+G4 and GTR+F+G4 for ND2 codon positions 1, 2 and 3, respectively.

Phylogenetic relationships were inferred through Maximum Likelihood (ML) and Bayesian Inference (BI). The ML analysis was performed using the IQ-TREE web-server 1.6.12 (Trifinopoulos et al. 2016) with 1,000 bootstrap pseudo-replicates using the ultrafast bootstrap analysis (Minh et al. 2013; Hoang et al. 2018). The BI analysis was implemented in MrBayes v.3.2 (Ronquist et al. 2012) on the CIPRES Science Gateway V. 3.3 (Miller et al. 2010) using default priors and models of evolution that were selected by ModelFinder and used in the ML analysis. Two independent runs, each with three heated and one cold chain, were performed using Markov Chain Monte Carlo (MCMC). The MCMC chains were run for 10,000,000 generations and trees sampled every 1,000 generations with the first 25% of each run discarded as burn-in. Stationarity was evaluated by ensuring effective sample sizes (ESS) were above 200 for all parameters in Tracer v. 1.7 (Rambaut et al. 2018). The phylogenetic trees from the ML and BI analyses were visualised using FigTree v. 1.4.4 (<http://tree.bio.ed.ac.uk/software/figtree/>). Nodes having ultrafast bootstrap support values (UFB) ≥ 95 and Bayesian posterior probabilities (BPP) ≥ 0.95 were considered well-supported (Huelsenbeck and Ronquist 2001; Wilcox et al. 2002; Minh et al. 2013). Uncorrected pairwise sequence divergences (*p*-distances) were calculated in MEGA 11 (Tamura et al. 2021) using the pairwise deletion option to remove gaps and missing data from the alignment prior to analysis.

Morphology

Morphological measurements were taken with digital calipers to the nearest 0.1 mm. Scalation and other aspects of external morphology were examined using a Nikon SMZ745 stereomicroscope. Measurements were taken on the left side of the body, while scale counts were taken on both right and left sides (R/L) when

possible. Morphological characters (measurements and meristics) and their abbreviations used follows Rujirawan et al. (2022): snout–vent length (**SVL**), taken from tip of snout to the anterior margin of vent; tail width (**TW**) at the base of the tail immediately posterior to the postcloacal swelling; tail length (**TL**), as distance from the vent to the tip of the tail, whether original, broken or regenerated; forearm length (**FL**), taken on the dorsal surface from the posterior margin of the elbow while flexed 90° to the inflection of the flexed wrist; tibia length (**TBL**), taken on the ventral surface from the posterior surface of the knee while flexed 90° to the base of the heel; head length (**HL**), as distance from the posterior margin of the retroarticular process of the lower jaw to the tip of the snout; head width (**HW**) at the angle of the jaws; head depth (**HD**), as the maximum height of head from the occiput to the throat; axilla-groin length (**AG**), taken from the posterior margin of the forelimb at its insertion point on the body to the anterior margin of the hind-limb at its insertion point on the body; eye diameter (**ED**), as the maximum horizontal diameter of the eyeball; eye-ear distance (**EE**), measured from the anterior margin of the ear opening to the posterior edge of the eyeball; ear length (**EL**), taken from the greatest vertical distance of the ear opening; eye-nostril distance (**EN**), measured from the anterior most margin of the eyeball to the posterior margin of the external nares; eye-snout distance (**ES**), measured from the anterior margin of the eyeball to the tip of snout; inner orbital distance (**IO**), as the width of the frontal bone at the level of the anterior edges of the orbit; internarial distance (**IN**), measured between the medial margins of the nares across the rostrum; supralabial scales (**SL**), counted from below the middle of the orbit to the rostral scale; infralabial scales (**IL**), counted from below the middle of the orbit to the mental scale; the number of paravertebral tubercles between limb insertions (**PVT**), counted in a straight line immediately left of the vertebral column; the number of subdigital lamellae beneath the fourth toe (**4TL**), counted from the base of the first phalanx to the claw; the total number of pore-bearing precloacal scales (**PP**) in males; and the number of postcloacal tubercles (**PCT**) on each side of tail base. Additional character states evaluated were the general size (i.e. strong, moderate, weak) and arrangement (i.e. random or linear) of the dorsal body tubercles; the orientation and shape of precloacal pores; the number of precloacal scales lacking pores separating the left and right series of pore-bearing precloacal scales; the degree and arrangement of body and tail tuberculation; the relative size and morphology of the subcaudal scales, subtibial scales and submetatarsal scales beneath the first metatarsal. Sex and maturity were determined by the presence of secondary sexual characteristics, such as the presence of hemipenes or pore-bearing precloacal scales in males, the presence of eggs in females or sexually dimorphic colour patterns. Morphological data for comparisons were obtained from the original and expanded descriptions of other species in the *C. siamensis* group (Smith 1925; Grismer and Chan 2010; Grismer et al. 2010, 2014, 2020; Wood et al. 2017; Ampai et al. 2019, 2020, 2022; Rujirawan et al. 2022).

Statistical analysis

All statistical analyses were conducted using R program v. 4.3.2 (R Core Team 2021). Morphospacial clustering and positioning among species was analysed using principal component analysis (PCA) in the FactoMineR and factoextra packages (Lê et al. 2008; Kassambara and Mundt 2020). Specimens of

three closely related species from Kanchanaburi Province were assigned to each group (= lineages, based on their mtDNA below), including, *C. auriventralis* ($n = 5$), *C. huaseesom* ($n = 3$) and the Wang Khrachae population ($n = 2$). For meristic characters, data were taken from the left side of examined specimens. Prior to the PCA analysis, fifteen morphometric characters (SVL, TW, FL, TBL, HL, HW, HD, AG, ED, EE, EL, EN, ES, IO, and IN) and four meristic characters (SL, IL, PVT, and 4TL) were concatenated into a single dataset. Precloacal pore (PP) was excluded from analyses due to their presence only in males. Tail length (TL) was excluded due to their different conditions (e.g., original, regenerated or broken). Postcloacal tubercle (PCT) was omitted due to inadequate data from *C. huaseesom*. To remove the effects of allometry, morphometric data (except SVL) were corrected for body-size variation using allometric growth model in the R package GroupStruct (available at <http://github.com/chankinonn/GroupStruct>) (Chan and Grismer 2022). Accordingly, the allometric formula is $X_{adj} = \log_{10}(X) - \beta[\log_{10}(SVL) - \log_{10}(SVL_{mean})]$, where X_{adj} = adjusted value; X = measured value; β = unstandardized regression coefficient for each population and SVL_{mean} = overall average SVL of all three populations (Thorpe 1975, 1983; Turan 1999; Lleonart et al. 2000).

Results

Phylogenetics

The final alignment of ND2 and flanking tRNAs contained 1,329 characters of 82 individuals of *Cnemaspis* and the outgroups. The ML and BI analyses recovered trees with topologies similar to each other and to those recovered by Ampai et al. (2022) and Rujirawan et al. (2022) (Fig. 2). The two samples from Wang Khrachae formed a well-supported monophyletic lineage (100 UFB, 1.00 BPP) and embed within the *C. siamensis* group. The Wang Khrachae population was recovered as the sister taxon (93 UFB, 1.00 BPP) to *C. huaseesom* from Sai Yok National Park, Sai Yok District, Kanchanaburi Province. Both lineages, the Wang Khrachae and *C. huaseesom* lineages, formed a clade as the sister taxon to *C. auriventralis* from Erawan National Park, Si Sawat District, Kanchanaburi Province. Uncorrected pairwise genetic divergence (p -distances) between the Wang Khrachae samples was 0.2%. The Wang Khrachae population had uncorrected p -distances of 8.3–9.4% from *C. huaseesom* and 11.3–24.5% from the remaining species of the *siamensis* group (Suppl. material 2). Uncorrected p -distances divergences within the *siamensis* group ranged from 6.8% (between *C. adangrawi* and *C. omari*) to 27.5% (between *C. roticanai* and *C. vandeventeri*).

The PCA analysis of three *Cnemaspis* lineages (the Wang Khrachae population, *C. auriventralis*, and *C. huaseesom*) from Kanchanaburi Province recovered morphological differences on a scatter plot of the first two PC axes (PC 1 and PC 2; Fig. 3). The first two axes accounted for 74.93% of cumulative of the total variation (50.36% for PC 1 axis and 24.58% for PC 2 axis; Table 1, Fig. 3). The factor loading of PC 1 was heavily loaded on most characters except HL and 4TL. The factor loading of PC 2 was heavily loaded on SVL, TW, TBL, HD, EN, ES, SL, PVT, and 4TL (Table 1). The PCA plot (first two axes) showed that the Wang Khrachae population is distinctly separated from *C. auriventralis* and *C. huaseesom* (Fig. 3). The *C. auriventralis* and *C. huaseesom* are also distinctly separated from each other.

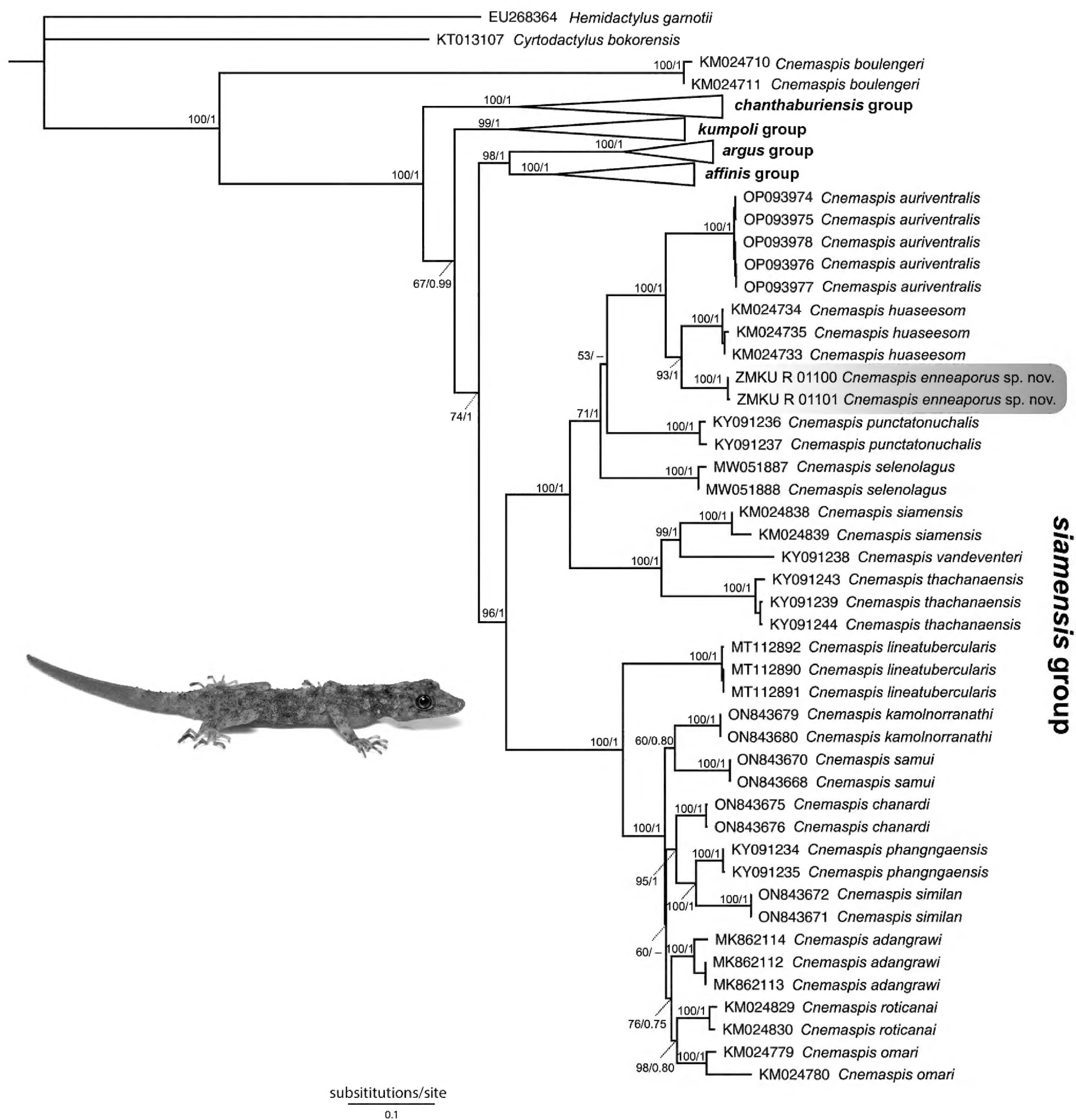


Figure 2. The best tree resulting from Maximum Likelihood analysis of 1,329 aligned characters of the mitochondrial NADH dehydrogenase subunit 2 gene and flanking tRNAs of *Cnemaspis* species. Nodal support is indicated by Ultrafast bootstrap (UFB) values and Bayesian posterior probabilities (BPP) from a separate Bayesian Inference analysis, respectively. GenBank accession numbers and locality data for sequenced samples are provided in Suppl. material 1.

Taxonomic hypotheses

The *Cnemaspis* samples from Wang Khrachae Subdistrict, Sai Yok District, Kanchanaburi Province differed from congeners in mtDNA analyses, multivariate analysis, and diagnostic morphological characters (see “Comparisons”). Based on these corroborating lines of evidence, we hypothesize that the Wang Khrachae population represents a previously unnamed species, which is described below.

Table 1. Factor loadings on the first five principal components (PC) of 19 morphological characters of *Cnemaspis enneaporus* sp. nov. and its closely related species, *C. auriventralis* and *C. huaseesom*. Morphological abbreviations are defined in Materials and methods.

Character	PC 1	PC 2	PC 3	PC 4	PC 5
SVL	0.8127	0.5248	0.08491	-0.08302	0.14543
TW	-0.5075	0.6983	-0.31075	0.24827	0.21863
FL	0.9096	0.3650	0.05729	-0.02468	0.04545
TBL	0.6322	-0.6381	-0.21347	-0.25227	0.14139
HL	0.2871	0.1055	0.90176	0.01232	-0.19016
HW	0.9572	-0.2027	-0.07465	-0.15252	0.00422
HD	0.7554	0.5998	-0.09544	0.09175	-0.04735
AG	0.9229	0.2483	-0.07096	0.06184	-0.15353
ED	0.7294	-0.0005	0.36329	-0.06324	0.50400
EE	0.6539	0.2684	-0.15147	-0.61508	-0.30723
EL	0.6080	0.2006	-0.23704	0.49270	-0.43409
EN	0.6812	0.6872	-0.01969	0.13057	0.19251
ES	0.6186	0.6850	-0.04838	0.02936	0.03754
IO	0.8802	-0.4025	-0.07851	0.00329	-0.15277
IN	0.9840	-0.0971	0.06670	-0.02101	0.03264
SL	0.5076	-0.7420	-0.27645	0.08171	0.08883
IL	0.5958	-0.4744	0.12948	0.60831	0.06261
PVT	-0.5957	0.5864	0.39654	-0.03285	-0.13491
4TL	-0.3375	0.7396	-0.38722	-0.08137	0.08159
Eigenvalue	9.568	4.669	1.610	1.196	0.789
Variance (%)	50.357	24.576	8.476	6.296	4.155
Cumulative variance (%)	50.357	74.933	83.409	89.705	93.860

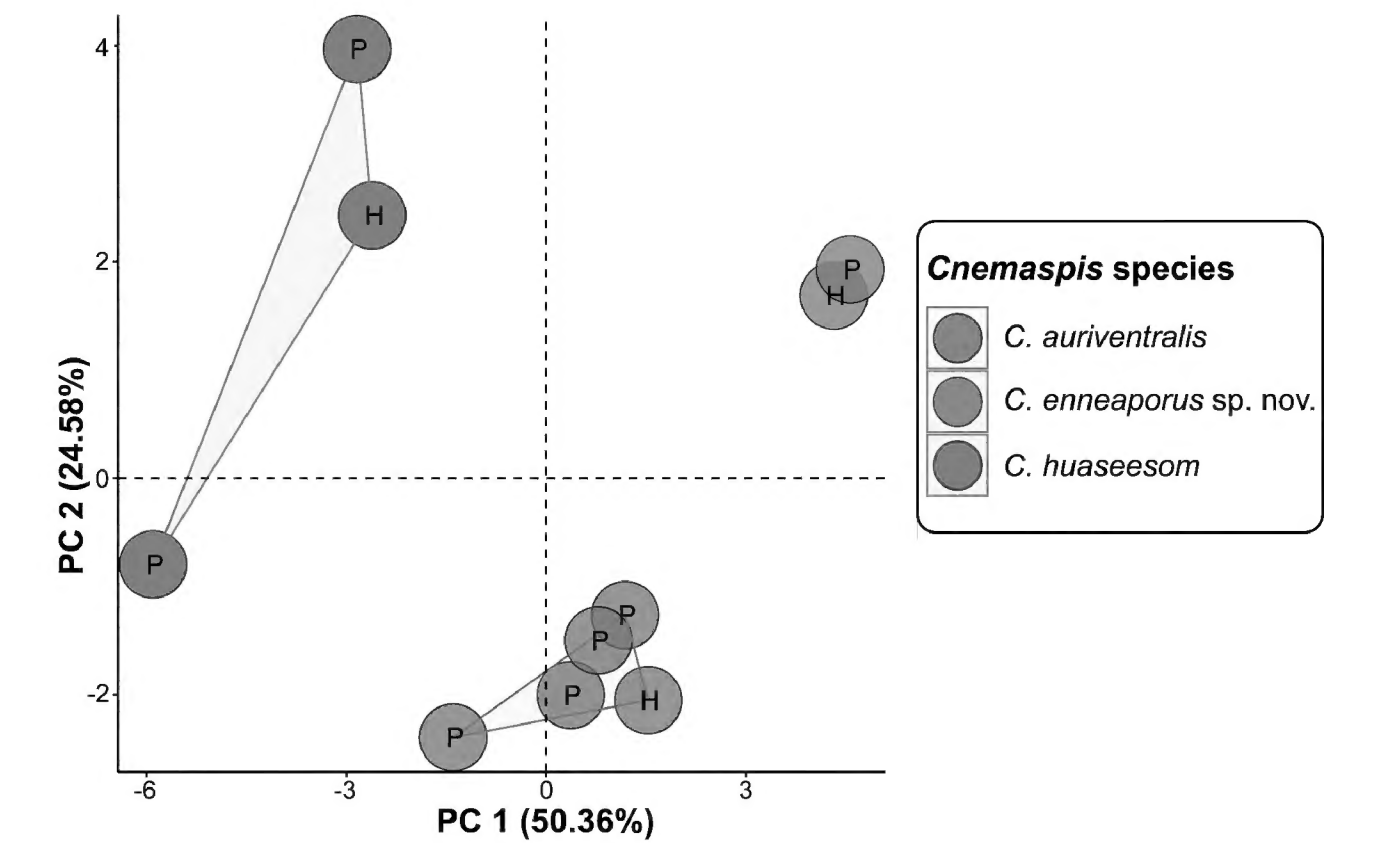


Figure 3. Plots of the first two principal components of *Cnemaspis enneaporus* sp. nov. and the closely related species based on 19 morphological characters. The letters in the scatter plots refer to holotype (H) and paratype (P).

Systematics

Cnemaspis enneaporus Rujirawan, Aksornneam & Aowphol, sp. nov.

<https://zoobank.org/7B95FC67-EC87-46F6-80D7-8062350F4917>

Figs 4–7

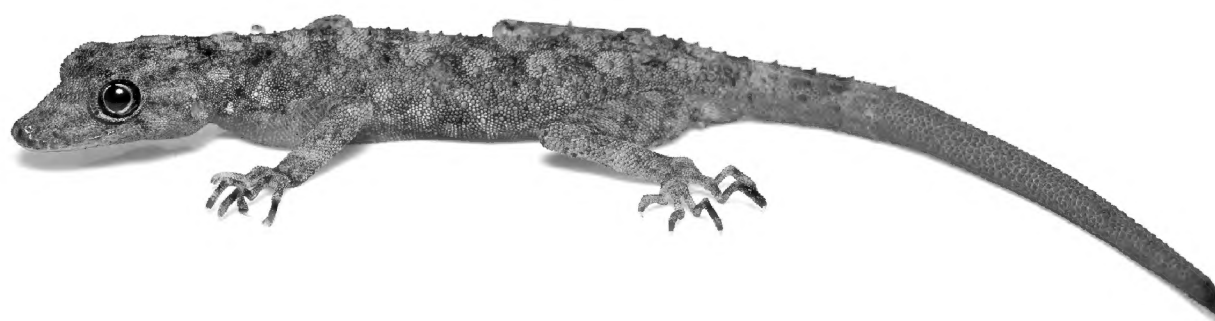
Type material. *Holotype* (Figs 4–6). ZMKU R 01100, adult male from Thailand, Kanchanaburi Province, Sai Yok District, Wang Khrachae Subdistrict, (14.20247°N, 99.02222°E; 404 m elevation), collected on 18 November 2022 by Akrachai Aksornneam and Parinya Pawangkhanant. *Paratype* (Fig. 7). ZMKU R 01101, adult female, same collection data as the holotype.

Diagnosis. *Cnemaspis enneaporus* sp. nov. can be distinguished from all other species in the *C. siamensis* group by having the unique combination of the following characters: SVL 42.2 mm in adult males ($n = 1$), 43.7 mm in adult females ($n = 1$); eight supralabials; seven or eight infralabials; ventral scales smooth; nine continuous precloacal pores in single male specimen; 17 or 18 paravertebral tubercles linearly arranged; tubercles on lower flanks present; lateral caudal furrows present; no caudal tubercles in the lateral furrows; ventrolateral caudal tubercles present on original portion of tail; caudal tubercles not encircling tail; subcaudals smooth; no enlarged median subcaudal row; two postcloacal tubercles on each side of tail; no shield-like subtibial scales; subtibial scales smooth; no enlarged submetatarsal scales; 26–28 subdigital lamellae on the fourth toe; sexually dimorphic for dorsal and ventral colour pattern; prescapular marking absent; gular marking absent; and yellow colouration in life on all ventral surfaces of head, body and tail in adult male.

Description of holotype. Adult male; SVL 42.2 mm; head oblong in dorsal profile, moderate in size (HL/SVL 0.29), somewhat narrow (HW/SVL 0.18), flat (HD/HL 0.38), distinct from neck; snout moderate (ES/HL 0.43), snout slightly concave in lateral profile; postnasal region concave medially; scales of rostrum round, smooth, raised, larger than similarly-shaped scales on occiput; weak supraorbital ridges; weak frontorostral sulcus; canthus rostralis smoothly rounded; eye large (ED/HL 0.21); extra-brillar fringe scales small in general, but larger anteriorly; pupil round; ear opening oval, taller than wide; rostral concave dorsally, dorsal 50% divided by longitudinal groove; rostral bordered posteriorly by supranasals, one large azygous internasal and nostrils; bordered laterally by first supralabials; 8R/8L (right/left) raised supralabials of similar size, but smallest posteriorly; 7R/8L infralabials, decreasing gradually in size posteriorly; nostrils small, elliptical, orientated dorsoposteriorly; bordered posteriorly by two flat postnasal scales; mental large, triangular, flat, extending to level of second infralabials, bordered posteriorly by two postmentals; mental slightly concave; gular scales smooth, flat, round or oval, juxtaposed; throat scales round, smooth, raised, juxtaposed to subimbricate.

Body slender, elongate (AG/SVL 0.44); small, raised, weakly keeled, dorsal scales generally equal in size throughout body, intermixed with numerous, large, multi-keeled, linearly arranged tubercles; enlarged, multi-keeled, conical tubercles on flanks; tubercles extend from the occiput to base of the tail and continue on tail in whorls; body tubercles slightly smaller anteriorly; 18 paravertebral

A



B

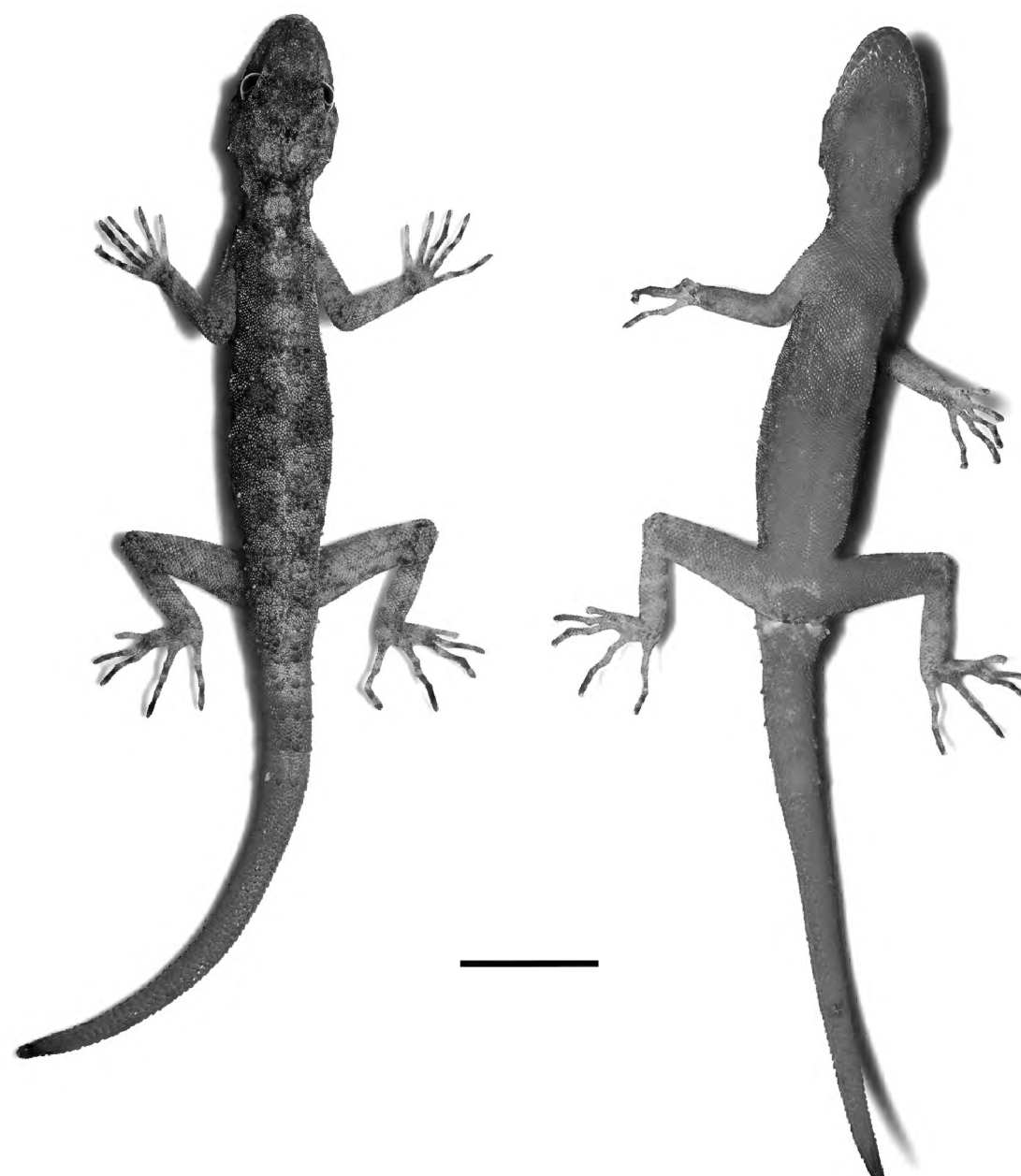


Figure 4. Adult male holotype of *Cnemaspis enneaporus* sp. nov. (ZMKU R 01100). **A** dorsolateral view in life **B** dorsal and ventral views immediately after euthanasia. Scale bar: 10 mm.

tubercles; pectoral and abdominal scales smooth, flat, imbricate; abdominal scales larger than pectoral and dorsal scales; nine contiguous, pore-bearing, precloacal scales; precloacal pores round to elongate.

Forelimbs moderately long, slender; dorsal scales raised, keeled, juxtaposed to subimbricate; ventral scales of brachia smooth, raised, juxtaposed to subimbricate; scales beneath forearm smooth, raised, subimbricate; digits long with an inflected joint; claws recurved; subdigital lamellae unnotched; subdigital lamellae wide throughout length of digits, bearing a larger scale at digital inflections; interdigital webbing absent; fingers increase in length from first to fifth, with fourth and fifth nearly equal in length; relative length of fingers $I < II < III < V \leq IV$; total subdigital lamellae on fingers I–V: 14–19–25–27–26 (right), 14–20–24–26–broken (left). Hind-limbs slightly longer and thicker than forelimbs; dorsal scales keeled, raised, juxtaposed; ventral scales of thigh and

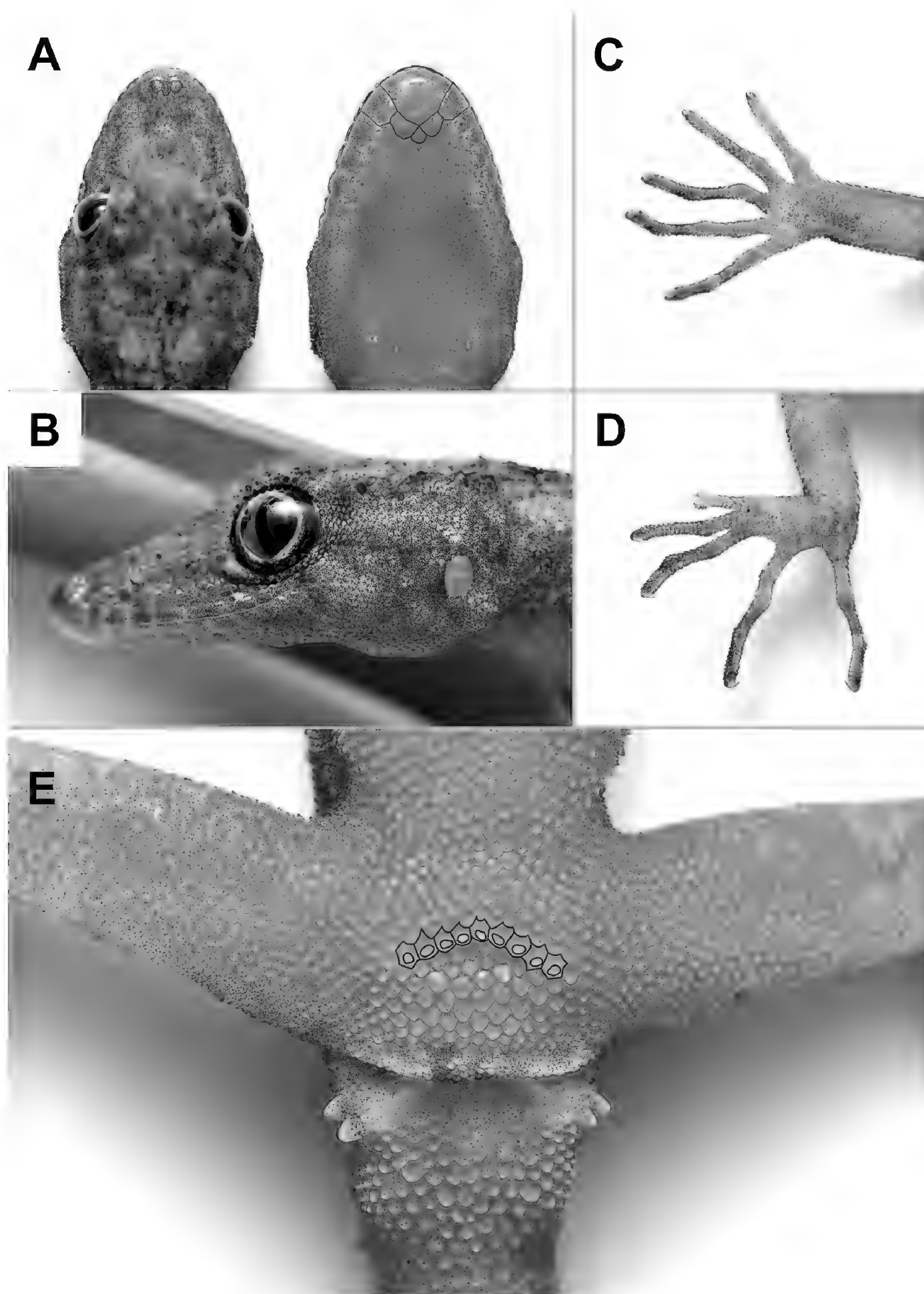


Figure 5. Adult male holotype of *Cnemaspis enneaporus* sp. nov. (ZMKU R 01100) immediately after euthanasia. **A** dorsal (supranasal and internasal scales outlined in black) and ventral views of head (mental, postmental, and first infralabial scales outlined in black) **B** lateral view of head **C** palmar view of the right manus **D** plantar view of the right pes **E** precloacal region with precloacal pores (outlined in black).

subtibial scales smooth, flat, imbricate; plantar scales smooth, slightly raised, subimbricate; enlarged submetatarsal scales beneath first toes absent; digits elongate with an inflected joint; claws recurved; subdigital lamellae unnotched; lamellae wide throughout length of digits; enlarged scales at digital inflections; interdigital webbing absent; toes increase in length from first to fourth and fifth nearly equal in length; relative length of toes $I < II < III < V \leq IV$; total subdigital lamellae on toes I–V: 13–18–23–28–25 (right), 13–18–26–28–26 (left).

Tail regenerated, long, slender, 42.1 mm in length (TL/SVL 1.00), tapering, becoming slender toward the tip; dorsal scales of the original portion of tail

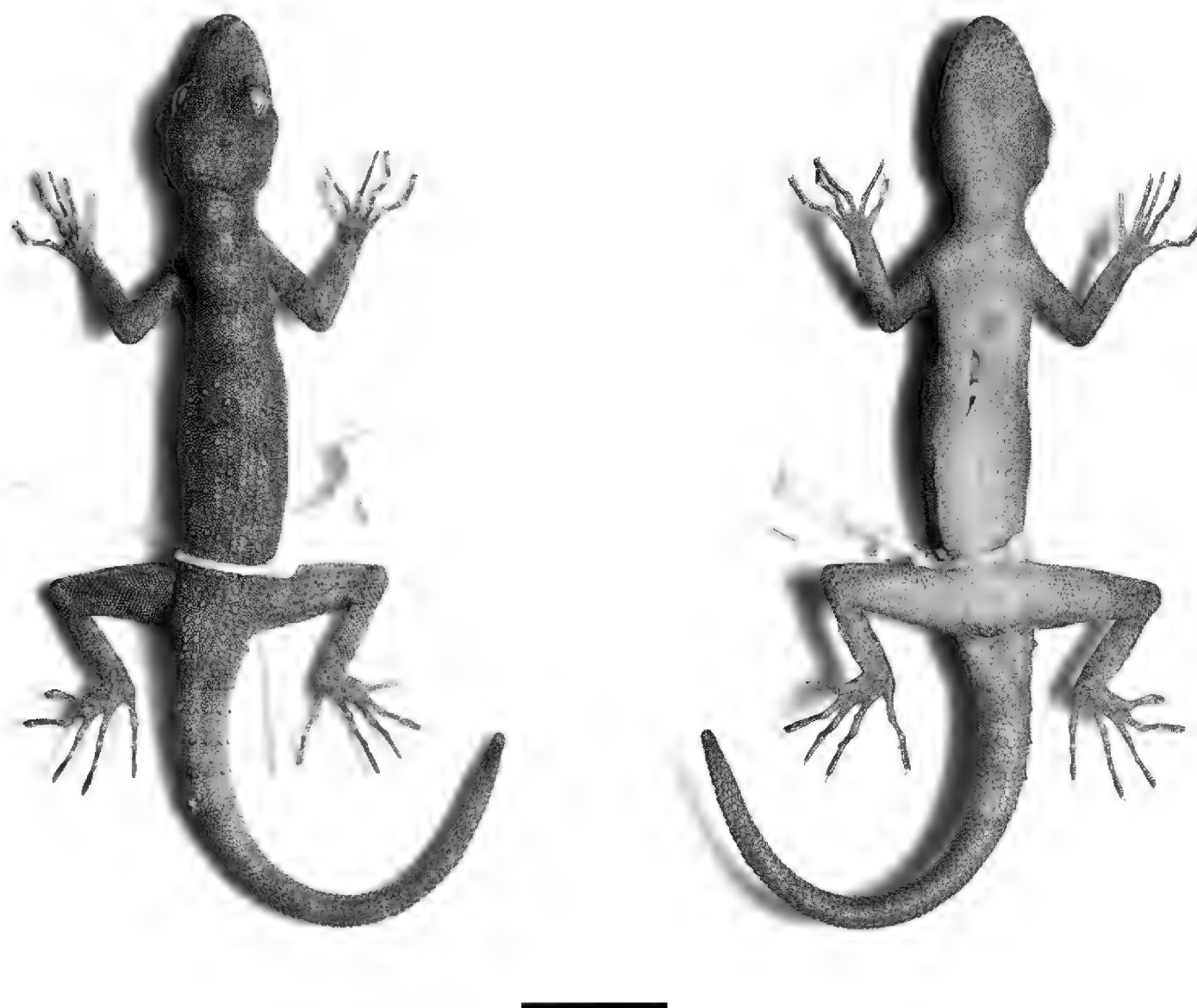


Figure 6. Dorsal and ventral views of adult male holotype of *Cnemaspis enneaporus* sp. nov. (ZMKU R 01100) in preservative. Scale bar: 10 mm.

slightly keeled, raised, juxtaposed, arranged in segmented whorls; mid-dorsal and lateral, caudal furrows present; subcaudals smooth, flat, imbricate; median row of enlarged subcaudal scales absent; paravertebral, dorsolateral and lateral rows of large, keeled, caudal tubercles extend length of original tail; ventrolateral rows of tubercles extend length of original tail; caudal tubercle rows do not encircle tail; tubercles absent from lateral caudal furrow; scale of the regenerated portion of tail smooth, flat, imbricate; enlarged postcloacal tubercles 2R/2L on lateral surface of hemipenial swellings at base of tail.

Colouration in life (Figs 4, 5). Dorsal ground colour of head, nape, trunk and limbs grey; dorsal ground colour of original and regenerate tail yellow; rostrum and interorbit regions bearing diffuse, faint, yellowish and brownish marking; top of head bearing small, diffuse, faint, dark, yellowish and light markings; dark postorbital stripes faint extending to occiput; pair of dark, diffuse, blotches on nape; large, light, irregularly-shaped, vertebral blotches extend from nape to base of tail, continuing on to original portion of tail as light yellow caudal bands; small, light, irregularly-shaped blotches in shoulder regions and flanks; limbs mottled with small, diffuse, dark marking; digits grey bearing dark bands. All ventral surfaces of head, body, thigh and original and regenerate portion of tail yellow; ventral surfaces of forelimbs and tibial region light grey with yellow speckling.

Colouration in preservative (Fig. 6). Dorsal and lateral surfaces of head, body, limbs and tail darker grey than in life, with some fading of markings. Ventral surfaces of head, body, limbs and tail creamy-white, with minute dark speckling on gular region, limbs and tail regions; regenerate portion of tail darker than original tail.

Variation. Variation in morphometric and meristic data between the holotype and paratype are presented in Table 2. *Cnemaspis enneaporus* sp. nov. shows

Table 2. Descriptive measurements (mm) and meristics (right/left) of the type series of *Cnemaspis enneaporus* sp. nov. Morphological abbreviations are defined in Materials and Methods.

Museum number	ZMKU R 01100	ZMKU R 01101
Type	holotype	paratype
Sex	male	female
SVL	42.2	43.7
TW	3.2	3.7
TL	42.1	6.3
Tail condition	regenerated	broken
FL	7.0	7.4
TBL	7.5	7.6
HL	12.2	11.5
HW	7.6	7.6
HD	4.6	4.7
AG	18.7	20.0
ED	2.6	2.3
EE	3.0	3.0
EL	1.3	1.3
EN	4.3	4.3
ES	5.2	5.2
IO	2.8	2.8
IN	1.3	1.2
HL/SVL	0.29	0.26
HW/SVL	0.18	0.17
HD/HL	0.38	0.41
ES/HL	0.43	0.45
ED/HL	0.21	0.20
AG/SVL	0.44	0.46
TL/SVL	1.00	0.14
Scalation		
SL	8R / 8L	8R / 8L
IL	7R / 8L	7R / 8L
PVT	18	17
4TL	28R / 28L	27R / 26L
PP	9 continuous	absent
PCT	2R / 2L	2R / 2L

significant sexual dimorphism in colour pattern. Yellow colouration on ventral surface of female (ZMKU R 01101) absent. Tail of the paratype is broken (TL = 6.3 mm) without yellow colouration of dorsal and ventral surface. The female paratype lack precloacal pores and has postcloacal tubercles that are relatively smaller than those in the male. Mental scale of the paratype bordered posteriorly by three post-mental scales. The paratype has skin swelling on left side of axillary area.

Distribution and natural history. The new species is known only from the type locality (Wang Khrachae Subdistrict, Sai Yok District, Kanchanaburi Province, Thailand) at ~ 400 m elevation in a karst formation that is part of the Tenasserim Mountain Range in western Thailand (Figs 1, 8). The holotype and paratype were found on karst boulders (~ 1.2–1.5 m height from ground) at night (00.00–00.30 h). One adult female (not collected; Fig. 8C) of *C. enneaporus* sp. nov. was found at the type locality on 31 August 2015 and was observed on a vine on a nearby karst wall

A



B

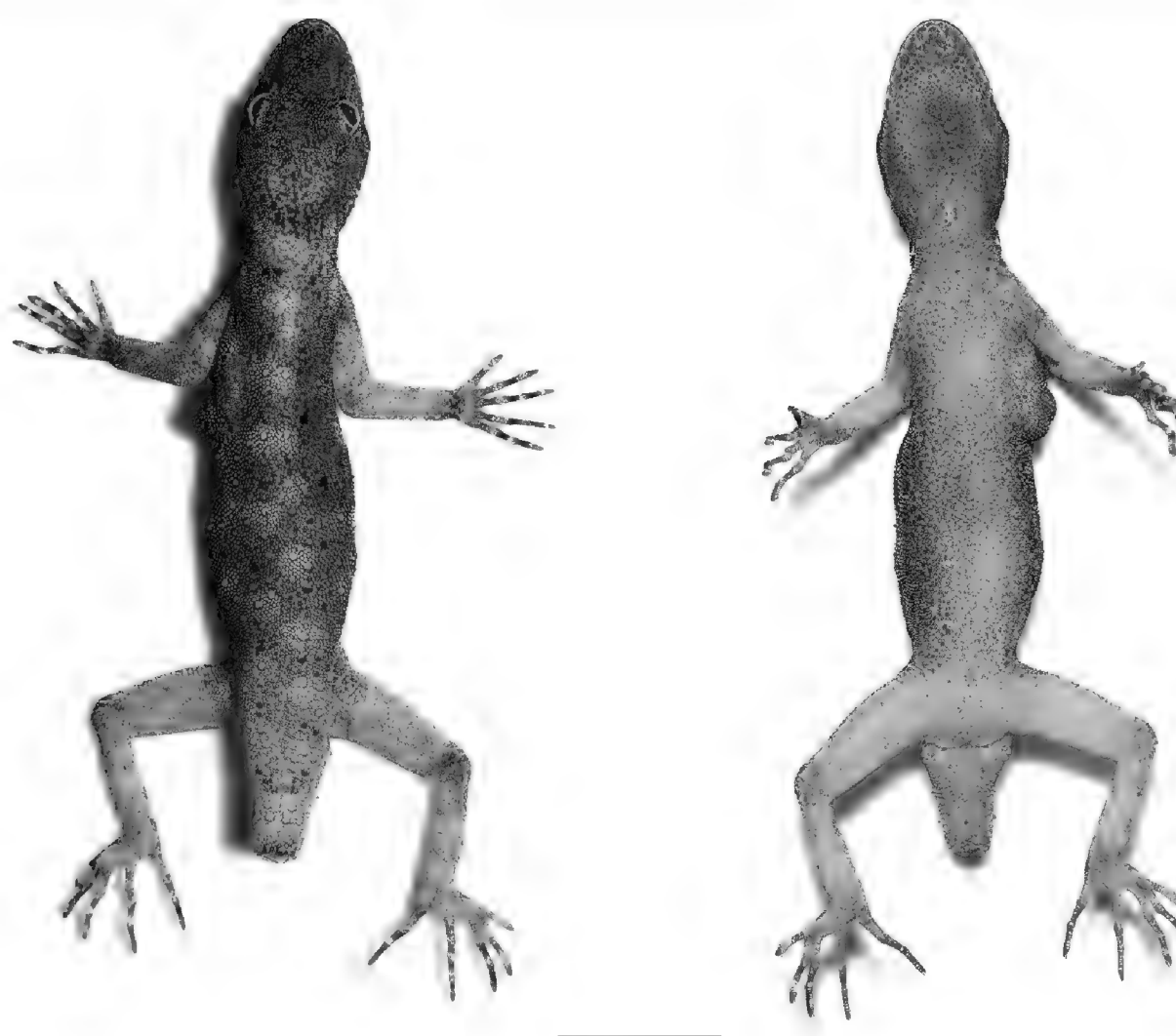


Figure 7. Adult female paratype of *Cnemaspis enneaporus* sp. nov. (ZMKU R 01101). **A** dorsolateral view in life **B** dorsal and ventral views immediately after euthanasia. Scale bar: 10 mm.

(~ 1.5 m height from ground) at night (23.00 h). Other species of reptiles observed in the type locality were *Cyrtodactylus saiyok* Panitvong, Sumontha, Tunprasert & Pauwels, 2014, *Cyrtodactylus tigroides* Bauer, Sumontha & Pauwels, 2003, *Gehyra mutilata* (Wiegmann, 1834), *Dixonius hangseesom* Bauer, Sumontha, Grossmann, Pauwels & Vogel, 2004, and *Trimeresurus kanburiensis* Smith, 1943.

Etymology. The species epithet *enneaporus* is derived from *ennea* (G.) for nine and *porus* (L.) for pore in reference to the male holotype of the new species having nine precloacal pores.

Suggested common name. Sai Yok Rock Gecko (English), Jing Jok Niew Yao Sai Yok (Thai).

Comparisons. *Cnemaspis enneaporus* sp. nov. is distinguishable from all other members of the *C. siamensis* group by a unique combination of morphological and colour pattern characteristics. *Cnemaspis enneaporus* sp. nov. differs from *C. adangrawi* Ampai, Rujirawan, Wood, Stuart & Aowphol,

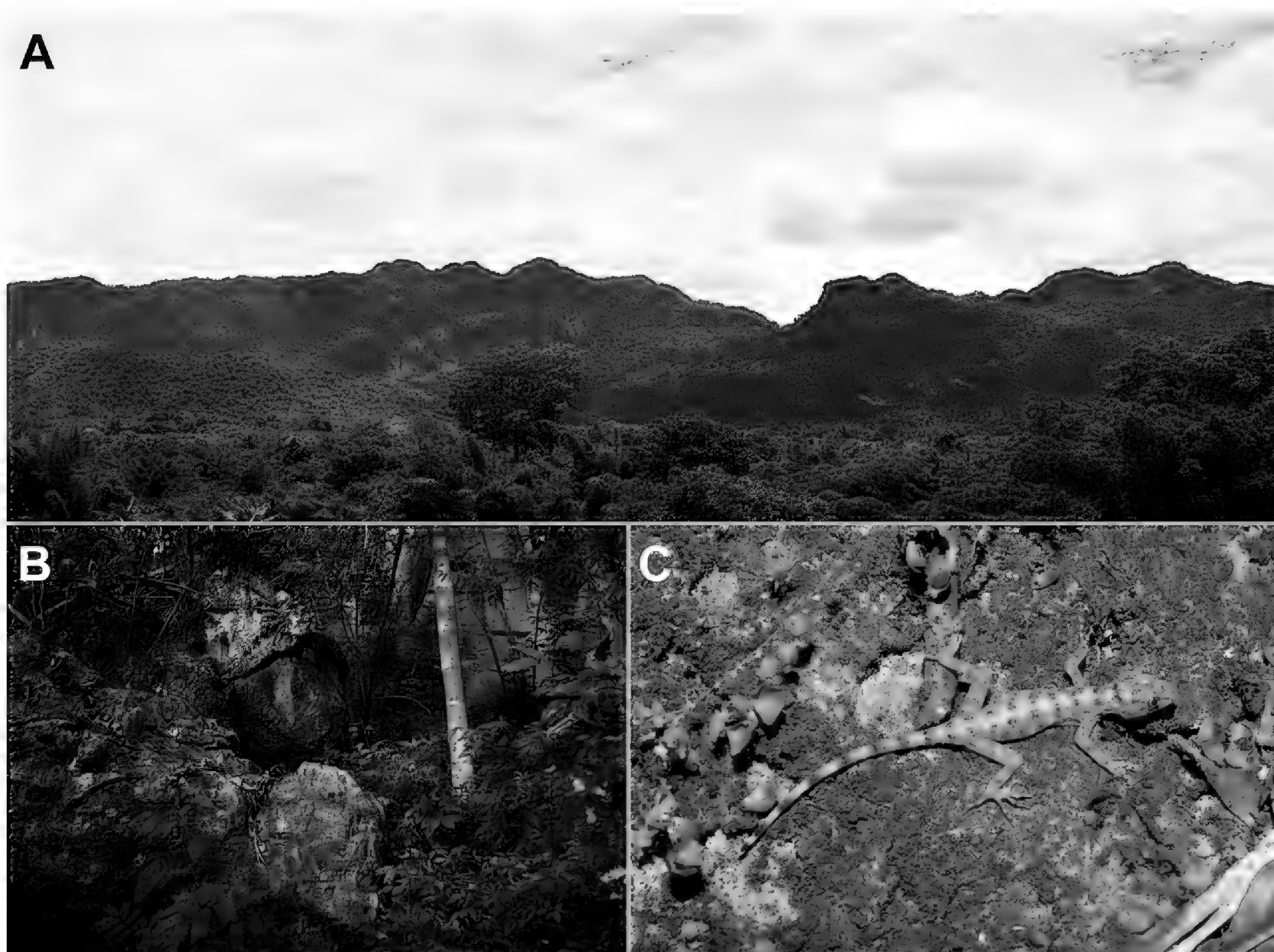


Figure 8. Habitat of *Cnemaspis enneaporus* sp. nov. at the type locality, Wang Khrachae Subdistrict, Sai Yok District, Kanchanaburi Province, Thailand. **A** landscape view of karst formation **B** karst microhabitat structure **C** adult female of *Cnemaspis enneaporus* sp. nov. (not collected) photographed *in situ* at the type locality.

2019 by having eight supralabials (vs 10); seven or eight infralabials (vs nine); ventral scales smooth (vs keeled); nine precloacal pores in male (vs 6–8 pores); precloacal pores continuous (vs separated); 17 or 18 paravertebral tubercles (vs 23–25 tubercles); paravertebral tubercles linearly arranged (vs randomly); tubercles on lower flanks present (vs absent); caudal tubercles in lateral furrow absent (vs present); subcaudal scales smooth (vs keeled); two postcloacal tubercles on each side in male (vs single tubercle); subtibial scales smooth (vs keeled); sexual dimorphism of dorsal colour pattern present (vs absent); light or yellowish prescapular crescent absent (vs present); yellow colouration on original and regenerated tail in male present (vs absent); and yellow colouration on all ventral surfaces of head, body and tail in male (vs yellowish colouration only on gular region, abdominal region and caudal region).

Cnemaspis enneaporus sp. nov. differs from *C. auriventralis* by having a larger maximum SVL of 43.7 mm (vs 38.6 mm); nine precloacal pores in male (vs 6 or 7 pores); and median row of subcaudal scales not enlarged (vs enlarged).

Cnemaspis enneaporus sp. nov. differs from *C. chanardi* Grismer, Sumontha, Cota, Grismer, Wood, Pauwels & Kunya, 2010 by having a larger maximum SVL of 43.7 mm (vs 40.1 mm); ventral scales smooth (vs keeled); nine precloacal pores in male (vs 6–8 pores); precloacal pores continuous (vs separated); 17 or 18 paravertebral tubercles (vs 22–25 tubercles); paravertebral tubercles linearly arranged (vs randomly); median row of subcaudal scales not enlarged (vs enlarged); subcaudal scales smooth (vs keeled); two postcloacal tubercles on

each side in male (vs single tubercle); subtibial scales smooth (vs keeled); sexual dimorphism of dorsal colour pattern present (vs absent); light or yellowish prescapular crescent absent (vs present); yellow colouration on original and regenerated tail in male present (vs absent); and yellow colouration on all ventral surfaces of head, body and tail in male (vs yellow colouration only on gular region, belly, underside of hindlimbs and subcaudal region).

Cnemaspis enneaporus sp. nov. differs from *C. huaseesom* by having nine precloacal pores in male (vs 5–8 pores); caudal tubercles in lateral furrow absent (vs present); yellow colouration on dorsal surface of head and forelimbs in males absent (vs present); yellow colouration on regenerated tail in male present (vs absent); and yellow colouration on all ventral surfaces of head, body and tail in male (vs yellow colouration only on gular region, throat, pectoral region, underside of forelimbs and subcaudal region).

Cnemaspis enneaporus sp. nov. differs from *C. kamolnorranathi* Grismer, Sumontha, Cota, Grismer, Wood, Pauwels & Kunya, 2010 by having a larger maximum SVL of 43.7 mm (vs 37.8 mm); nine precloacal pores in male (vs seven pores); 17 or 18 paravertebral tubercles (vs 19–24 tubercles); caudal tubercles in lateral furrow absent (vs present); subcaudal scales smooth (vs keeled); sexual dimorphism of dorsal colour pattern present (vs absent); yellow colouration on original and regenerated tail in male present (vs absent); and yellow colouration on all ventral surfaces of head, body and tail in male (vs lacking yellow colouration on ventral surfaces).

Cnemaspis enneaporus sp. nov. differs from *C. lineatubercularis* Ampai, Wood, Stuart & Aowphol, 2020 by having ventral scales smooth (vs keeled); 17 or 18 paravertebral tubercles (vs 19–21); subcaudal scales smooth (vs keeled); two postcloacal tubercles on each side in male (vs single tubercle); subtibial scales smooth (vs keeled); sexual dimorphism of dorsal colour pattern present (vs absent); light or yellowish prescapular crescent absent (vs present); yellow colouration on original and regenerated tail in male present (vs absent); and yellow colouration on all ventral surfaces of head, body and tail in male (vs yellowish colouration only on anterior gular, abdominal and subcaudal regions).

Cnemaspis enneaporus sp. nov. differs from *C. omari* Grismer, Wood, Anuar, Riyanto, Ahmad, Muin, Sumontha, Grismer, Chan, Quah & Pauwels, 2014 by having ventral scales smooth (vs keeled); nine precloacal pores in male (vs 4 pores); precloacal pores continuous (vs separated); 17 or 18 paravertebral tubercles (vs 22–29 tubercles); caudal tubercles not encircling the tail (vs encircling); two postcloacal tubercles on each side in male (vs single tubercle); subtibial scales smooth (vs keeled); sexual dimorphism of dorsal colour pattern present (vs absent); light or yellowish prescapular crescent absent (vs present); yellow colouration on original and regenerated tail in male present (vs absent); and yellow colouration on all ventral surfaces of head, body and tail in male (vs yellow colouration only on gular region, belly, underside of hind-limbs, and subcaudal region).

Cnemaspis enneaporus sp. nov. differs from *C. phangngaensis* Wood, Grismer, Aowphol, Aguilar, Cota, Grismer, Murdoch & Sites, 2017 by having eight supralabials (vs 10); seven or eight infralabials (vs 10); ventral scales smooth (vs keeled); nine precloacal pores in male (vs 4 pores); 17 or 18 paravertebral tubercles (vs 22 tubercles); tubercles on lower flanks present (vs absent); subcaudal scales smooth (vs keeled); subtibial scales smooth (vs keeled);

26–28 subdigital lamellae on the fourth toe (vs 29 lamellae); light or yellowish prescapular crescent absent (vs present); yellow colouration on original and regenerated tail in male present (vs absent); and yellow colouration on all ventral surfaces of head, body and tail in male (vs yellow colouration only on anterior gular region, abdomen and subcaudal region).

Cnemaspis enneaporus sp. nov. differs from *C. punctatonuchalis* Grismer, Sumontha, Cota, Grismer, Wood, Pauwels & Kunya, 2010 by having a smaller maximum SVL of 43.7 mm (vs 49.6 mm); nine precloacal pores in male (vs absent); 17 or 18 paravertebral tubercles (vs 24–27); median row of subcaudal scales not enlarged (vs enlarged); 26–28 subdigital lamellae on the fourth toe (vs 29–31 lamellae); ocelli on brachium and side of neck in male absent (vs present); yellow colouration on original tail in male present (vs absent); and yellow colouration on all ventral surfaces of body and tail in male (vs orange colouration on throat and subcaudal region).

Cnemaspis enneaporus sp. nov. differs from *C. roticanai* Grismer & Chan, 2010 by having a smaller maximum SVL of 43.7 mm (vs 47.0 mm); ventral scales smooth (vs keeled); nine precloacal pores in male (vs 3–6 pores); 17 or 18 paravertebral tubercles (vs 25–27 tubercles); paravertebral tubercles linearly arranged (vs randomly); median row of subcaudal scales not enlarged (vs enlarged); subcaudal scales smooth (vs keeled); subtibial scales smooth (vs keeled); light or yellowish prescapular crescent absent (vs present); and yellow colouration on original tail in male present (vs absent).

Cnemaspis enneaporus sp. nov. differs from *C. samui* Ampai, Rujirawan, Yodthong, Termprayoon, Stuart, Wood & Aowphol, 2022 by having ventral scales smooth (vs keeled); nine precloacal pores in male (vs 5–8 pores); precloacal pores continuous (vs separated); 17 or 18 paravertebral tubercles (vs 25–27 tubercles); paravertebral tubercles linearly arranged (vs randomly); median row of subcaudal scales not enlarged (vs enlarged); subcaudal scales smooth (vs keeled); subtibial scales smooth (vs keeled); 26–28 subdigital lamellae on the fourth toe (vs 22–25 lamellae); sexual dimorphism of dorsal colour pattern present (vs absent); light or yellowish prescapular crescent absent (vs present); yellow colouration on original and regenerated tail in male present (vs absent); and yellow colouration on all ventral surfaces of head, body and tail in male (vs yellowish colouration only on gular region, abdomen, limbs and subcaudal region).

Cnemaspis enneaporus sp. nov. differs from *C. selenolagus* Grismer, Yushchenko, Pawangkhanant, Nazarov, Naiduangchan, Suwannapoom & Poyarkov, 2020 by having a larger maximum SVL of 43.7 mm (vs 36.2 mm); eight supralabials (vs 10–11); seven or eight infralabials (vs 10); nine precloacal pores in male (vs six or seven pores); paravertebral tubercles linearly arranged (vs randomly); tubercles on lower flanks present (vs absent); lateral caudal furrow present (vs absent); caudal tubercles not encircling the tail (vs encircling); enlarged submetatarsal scales on the first toe absent (vs present); 26–28 subdigital lamellae on the fourth toe (vs 22 lamellae); orange-yellow colouration on anterior 1/2 of body in male absent (vs present); ocelli on brachium and side of neck in males absent (vs present); light or yellowish prescapular crescent absent (vs present); yellow colouration on dorsal surface of forelimbs in male absent (vs present); yellow colouration on original and regenerated tail in male present (vs absent); and yellow colouration on all ventral surfaces of head, body and tail in male (vs yellow colouration only on anterior part of body).

Cnemaspis enneaporus sp. nov. differs from *C. siamensis* (Smith, 1925) by having a larger maximum SVL of 43.7 mm (vs 39.7 mm); ventral scales smooth (vs keeled); nine precloacal pores in male (vs absent); 17 or 18 paravertebral tubercles (vs 19–25 tubercles); paravertebral tubercles linearly arranged (vs randomly); median row of subcaudal scales not enlarged (vs enlarged); subcaudal scales smooth (vs keeled); subtibial scales smooth (vs keeled); sexual dimorphism of dorsal colour pattern present (vs absent); yellow colouration on original and regenerated tail in male present (vs absent); lineate gular marking absent (vs present); and yellow colouration on all ventral surfaces of head, body and tail in males (vs yellow colouration only on gular region, throat and pectoral region).

Cnemaspis enneaporus sp. nov. differs from *C. similan* Ampai, Rujirawan, Yodthong, Termprayoon, Stuart, Wood & Aowphol, 2022 by having a smaller maximum SVL of 43.7 mm (vs 48.1 mm); ventral scales smooth (vs keeled); nine precloacal pores in male (vs one pore); 17 or 18 paravertebral tubercles (vs 24 or 25 tubercles); paravertebral tubercles linearly arranged (vs randomly); subcaudal scales smooth (vs keeled); subtibial scales smooth (vs keeled); 26–28 subdigital lamellae on the fourth toe (vs 23 or 24 lamellae); light or yellowish prescapular crescent absent (vs present); yellow colouration on original and regenerated tail in male present (vs absent); and yellow colouration on all ventral surfaces of head, body and tail in male (vs pale yellowish blotches or reticulum on gular, neck, limbs and belly).

Cnemaspis enneaporus sp. nov. differs from *C. thachanaensis* Wood, Grismer, Aowphol, Aguilar, Cota, Grismer, Murdoch & Sites, 2017 by having a larger maximum SVL of 43.7 mm (vs 39.0 mm); eight supralabials (vs 10 or 11); seven or eight infralabials (vs nine or 11); ventral scales smooth (vs keeled); nine precloacal pores in male (vs absent); subcaudal scales smooth (vs keeled); two postcloacal tubercles on each side in male (vs absent); subtibial scales smooth (vs keeled); enlarged submetatarsal scales on the first toe absent (vs present); 26–28 subdigital lamellae on the fourth toe (vs 23–25 lamellae); yellow colouration on original and regenerated tail in male present (vs absent); lineate gular marking absent (vs present); and yellow colouration on all ventral surfaces of head, body and tail in male (vs yellowish-orange colouration only on gular region).

Cnemaspis enneaporus sp. nov. differs from *C. vandeventeri* Grismer, Sumontha, Cota, Grismer, Wood, Pauwels & Kunya, 2010 by having ventral scales smooth (vs keeled); nine precloacal pores in male (vs four pores); 17 or 18 paravertebral tubercles (vs 25–29 tubercles); paravertebral tubercles linearly arranged (vs randomly); tubercles on lower flanks present (vs absent); median row of subcaudal scales not enlarged (vs enlarged); subcaudal scales smooth (vs keeled); subtibial scales smooth (vs keeled); sexual dimorphism of dorsal colour pattern present (vs absent); light or yellowish prescapular crescent absent (vs present); yellow colouration on original and regenerated tail in male present (vs absent); and yellow colouration on all ventral surfaces of head, body and tail in male (vs orange colouration on gular region, throat, pectoral region, underside of limbs, belly and subcaudal region).

Discussion

Cnemaspis enneaporus sp. nov. superficially resembles *C. auriventralis* from Erawan National Park in colouration pattern of adult male (yellow colouration on all ventral surface of head, body and subcaudal regions). However, the

new species is closely related to *C. huaseesom* from Sai Yok National Park and these two species form the sister clade to *C. auriventralis* from Erawan National Park. These three species were found in similar habitat (karst-associated area) in Kanchanaburi Province, western Thailand. Moreover, the type locality of the new species is ca 20 km and 30 km from *C. auriventralis* and *C. huaseesom*, respectively. However, the combination of morphology, phylogenetic position and high genetic divergences (8.3–11.9%) revealed clear differences among them. Unfortunately, the new species is known from only two specimens (one individual was not collected; Fig. 8C) from the type locality at ~ 400 m elevation. During January 2018 and February 2019, Aksornneam et al. (2023) conducted ecological surveys of two sympatric geckos, *Cyrt. saiyok* and *Cyrt. tigroides* in the karst habitats within the type locality of *C. enneaporus* sp. nov. at elevation ranging from 250–350 m. The new species was not observed during their study or in previous surveys conducted below 350 m elevation (AAK and AR pers. obs.). This suggests that the geographic distribution of the new species could be limited by elevation (above 400 m). However, the highest elevation surveyed was ca 500 m (AAK pers. obs.), while the peak of the karst hill is ca 800 m. Additional surveys at higher and lower elevations are needed to better understand the ecological niche and microhabitats of the new species.

The description of *C. enneaporus* sp. nov. brings the total number of Thai *Cnemaspis* species to 24 (23 Southeast Asian clade members + 1 South Asian clade member) and the number of species in the *siamensis* group to 17 (Ampai et al. 2022; Rujirawan et al. 2022; Uetz et al. 2024). Karst or limestone areas are special and spectacular types of landscapes created by the dissolution of carbonate rocks, consisting of a diverse array of microhabitats shaped by complex terrains and variable climatic conditions (Clements et al. 2006; van Beynen 2011; Jantarit and Ellis 2023). In Thailand, karst landscape covers ~ 18% of the land area (ca 93,000 km²) and the largest karst area in the country (covering ca 12,00 km²) is in Kanchanaburi Province, western region (Sidisunthorn et al. 2006; Bolger and Ellis 2015; Jantarit and Ellis 2023). Previously, several herpetofauna species, which are apparently restricted to karst habitats, were discovered from Kanchanaburi Province i.e. *C. auriventralis*, *C. huaseesom*, *Cyrtodactylus monilatus* Yodthong, Rujirawan, Stuart, Grismer, Aksornneam, Termprayoon, Ampai & Aowphol, 2022, *Cyrtodactylus fluvicavus* Grismer, Aowphol, Yodthong, Ampai, Termprayoon, Aksornneam & Rujirawan, 2022, *Cyrt. tigroides*, *D. hangseesom*, *Gekko nutaphandi* Bauer, Sumontha & Pauwels, 2008, *Oligodon saiyok* Sumontha, Kunya, Dangsri & Pauwels, 2017, *Siamophryne troglodytes* Suwannapoom, Sumontha, Tunprasert, Ruangsuwan, Pawangkhanant, Korost & Poyarkov, 2018, and *T. kanburiensis* (Smith 1943; Bauer et al. 2003, 2004, 2008; Sumontha et al. 2017; Suwannapoom et al. 2018; Grismer et al. 2022; Rujirawan et al. 2022; Yodthong et al. 2022). The discovery of the new species of *Cnemaspis* in association with karst underscores the significance of the karst habitats in Kanchanaburi for herpetofauna diversity and endemism within Thailand. It also highlights the need for additional field surveys in the karst formations along the northern part of the Tenasserim Mountain Range in western Thailand to determine the total geographic range of *C. enneaporus* sp. nov. and its closely relatives and enhance the documentation of herpetofauna diversity in Thailand.

Acknowledgements

We would like to thank Jitthep Tunprasert, Mali Naiduangchan and Kenneth Chin for assisting in fieldwork. AR was supported by International SciKU Branding (ISB), Faculty of Science, Kasetsart University. AAK and PP were supported by the Rabbit in the Moon Foundation. We thanks to Ishan Agarwal and an anonymous reviewer for their valuable comments, which improved the manuscript.

Additional information

Conflict of interest

The authors have declared that no competing interests exist.

Ethical statement

This research was approved by the Institutional Animal Care and Use Committee of the Faculty of Science, Kasetsart University (AKU67-SCI-009).

Funding

This research has received funding support from the NSRF via the Program Management Unit for Human Resources & Institutional Development, Research and Innovation [grant number B42G670038].

Author contributions

Conceptualization: AR, AAO. Data curation: AR. Formal analysis: AR, AAO. Funding acquisition: AAO. Investigation: AAK, PP, BLS, SY, AAO, AR. Methodology: AR, BLS, AAO, AAK, SY, PP. Project administration: AAO. Supervision: AAO, AR. Validation: AR. Visualization: AAK, AR. Writing - original draft: AR, AAO. Writing – review and editing: PP, AR, AAK, BLS, SY, AAO.

Author ORCIDs

Attapol Rujirawan  <https://orcid.org/0000-0001-9179-6910>

Akrachai Aksornneam  <https://orcid.org/0000-0003-4780-376X>

Siriporn Yodthong  <https://orcid.org/0000-0001-6577-5358>

Parinya Pawangkhanant  <https://orcid.org/0000-0002-0947-5729>

Bryan L. Stuart  <https://orcid.org/0000-0003-4719-1951>

Anchalee Aowphol  <https://orcid.org/0000-0001-9504-4601>

Data availability

All of the data that support the findings of this study are available in the main text or Supplementary Information.

References

- Aksornneam A, Sung YH, Aowphol A (2023) Effect of habitat structure on abundance and body conditions of two sympatric geckos, *Cyrtodactylus saiyok* and *Cyrtodactylus tigroides*, in the karst forest of western Thailand. *Journal of Natural History* 57(5–8): 395–407. <https://doi.org/10.1080/00222933.2023.2186808>
- Ampai N, Rujirawan A, Wood Jr PL, Stuart BL, Aowphol A (2019) Morphological and molecular analyses reveal two new insular species of *Cnemaspis* Strauch, 1887 (Squa-

- mata, Gekkonidae) from Satun Province, southern Thailand. ZooKeys 858: 127–161. <https://doi.org/10.3897/zookeys.858.34297>
- Ampai N, Wood Jr PL, Stuart BL, Aowphol A (2020) Integrative taxonomy of the rock-dwelling gecko *Cnemaspis siamensis* complex (Squamata, Gekkonidae) reveals a new species from Nakhon Si Thammarat Province, southern Thailand. ZooKeys 932: 129–159. <https://doi.org/10.3897/zookeys.932.50602>
- Ampai N, Rujirawan A, Yodthong S, Termprayoon K, Stuart BL, Wood Jr PL, Aowphol A (2022) Hidden diversity of rock geckos within the *Cnemaspis siamensis* species group (Gekkonidae, Squamata): genetic and morphological data from southern Thailand reveal two new insular species and verify the phylogenetic affinities of *C. chanardi* and *C. kamolnorranathi*. ZooKeys 1125: 115–158. <https://doi.org/10.3897/zookeys.1125.94060>
- Bauer AM, Sumontha M, Pauwels OSG (2003) Two new species of *Cyrtodactylus* (Reptilia: Squamata: Gekkonidae) from Thailand. Zootaxa 376(1): 1–18. <https://doi.org/10.11646/zootaxa.376.1.1>
- Bauer AM, Sumontha M, Grossmann W, Pauwels OSG, Vogel G (2004) A new species of *Dixonius* (Squamata: Gekkonidae) from Kanchanaburi Province, western Thailand. Current Herpetology 23(1): 17–26. <https://doi.org/10.5358/hsj.23.17>
- Bauer AM, Sumontha M, Pauwels OSG (2008) A new red-eyed Gekko (Reptilia: Gekkonidae) from Kanchanaburi Province, Thailand. Zootaxa 1750(1): 32–42. <https://doi.org/10.11646/zootaxa.1750.1.3>
- Bolger T, Ellis M (2015) An overview of caves and caving in Thailand. Asian Transkarst Conference, Lichuan, Hubei, China, November 2015. Proceedings, Lichuan, 203–207.
- Chan KO, Grismer LL (2022) GroupStruct: an R package for allometric size correction. Zootaxa 5124(4): 471–482. <https://doi.org/10.11646/zootaxa.5124.4.4>
- Clements R, Sodhi NS, Schilthuizen M, Ng PKL (2006) Limestone karsts of Southeast Asia: imperiled arks of biodiversity. BioScience 56(9): 733–742. [https://doi.org/10.1641/0006-3568\(2006\)56\[733:LKOSAI\]2.0.CO;2](https://doi.org/10.1641/0006-3568(2006)56[733:LKOSAI]2.0.CO;2)
- Grismer LL, Chan KO (2010) Another new rock gecko (genus *Cnemaspis* Strauch 1887) from Pulau Langkawi, Kedah, Peninsular Malaysia. Zootaxa 2419(1): 51–62. <https://doi.org/10.11646/zootaxa.2419.1.2>
- Grismer LL, Sumontha M, Cota M, Grismer JL, Wood Jr PL, Pauwels OSG, Kunya K (2010) A revision and redescription of the rock gecko *Cnemaspis siamensis* (Taylor 1925) (Squamata: Gekkonidae) from Peninsular Thailand with descriptions of seven new species. Zootaxa 2576(1): 1–55. <https://doi.org/10.11646/zootaxa.2576.1.1>
- Grismer LL, Wood Jr PL, Anuar S, Riyanto A, Ahmad N, Muin MA, Sumontha M, Grismer JL, Chan KO, Quah ESH, Pauwels OSG (2014) Systematics and natural history of Southeast Asian Rock Geckos (genus *Cnemaspis* Strauch, 1887) with descriptions of eight new species from Malaysia, Thailand, and Indonesia. Zootaxa 3880(1): 1–147. <https://doi.org/10.11646/zootaxa.3880.1.1>
- Grismer LL, Yushchenko PV, Pawangkhanant P, Nazarov RA, Naiduangchan M, Suwanapoom C, Poyarkov NA (2020) A new species of *Cnemaspis* Strauch (Squamata: Gekkonidae) of the *C. siamensis* group from Tenasserim Mountains, Thailand. Zootaxa 4852(5): 547–564. <https://doi.org/10.11646/zootaxa.4852.5.3>
- Grismer LL, Aowphol A, Yodthong S, Ampai N, Termprayoon K, Aksornneam A, Rujirawan A (2022) Integrative taxonomy delimits and diagnoses cryptic arboreal species of the *Cyrtodactylus brevipalmatus* group (Squamata, Gekkonidae) with descriptions of four new species from Thailand. ZooKeys 1129: 109–162. <https://doi.org/10.3897/zookeys.1129.90535>

- Hoang DT, Chernomor O, von Haeseler A, Minh BQ, Vinh LS (2018) UFBoot2: Improving the ultrafast bootstrap approximation. *Molecular Biology and Evolution* 35(2): 518–522. <https://doi.org/10.1093/molbev/msx281>
- Huelsenbeck JP, Ronquist F (2001) MRBAYES: Bayesian inference of phylogenetic trees. *Bioinformatics* 17(8): 754–755. <https://doi.org/10.1093/bioinformatics/17.8.754>
- Jantarit S, Ellis M (2023) The cave fauna of Thailand. Prince of Songkla University Press, Songkhla, 396 pp.
- Kalyaanamoorthy S, Minh BQ, Wong TKF, von Haeseler A, Jermiin LS (2017) ModelFinder: fast model selection for accurate phylogenetic estimates. *Nature Methods* 14: 587–589. <https://doi.org/10.1038/nmeth.4285>
- Karunaratna S, Ukuwela KDB, De Silva A, Bauer AM, Madawala M, Poyarkov NA, Botejue M, Gabadage D, Grismer LL, Gorin VA (2023) A phylogenetic and taxonomic assessment of the *Cnemaspis alwisi* group (Reptilia: Gekkonidae) in Sri Lanka with a description of two new species from isolated misty-mountains. *Vertebrate Zoology* 73: 205–236. <https://doi.org/10.3897/vz.73.e90979>
- Kassambara A, Mundt F (2020) factoextra: extract and visualize the results of multivariate data analyses. R package version 1.0.7. <https://CRAN.R-project.org/package=factoextra>
- Katoh K, Standley DM (2013) MAFFT multiple sequence alignment software version 7: improvements in performance and usability. *Molecular Biology and Evolution* 30(4): 772–780. <https://doi.org/10.1093/molbev/mst010>
- Kurita T, Nishikawa K, Hossman MY, Mizuno T, Sato H, Gumal M (2024) Description of a new sandstone-dwelling species of genus *Cnemaspis* (Sauria: Gekkonidae) from Gunung Santubong National Park, southwestern Sarawak, Malaysia. *Zootaxa* 5468(2): 361–378. <https://doi.org/10.11646/zootaxa.5468.2.7>
- Lê S, Josse J, Husson F (2008) FactoMineR: an R package for multivariate analysis. *Journal of Statistical Software* 25(1):1–18. <https://doi.org/10.18637/jss.v025.i01>
- Lleonart J, Salat J, Torres GJ (2000) Removing allometric effects of body size in morphological analysis. *Journal of Theoretical Biology* 205(1): 85–93. <https://doi.org/10.1006/jtbi.2000.2043>
- Macey JR, Larson A, Ananjeva NB, Papenfuss TJ (1997) Evolutionary shifts in three major structural features of the mitochondrial genome among iguanian lizards. *Journal of Molecular Evolution* 44: 660–674. <https://doi.org/10.1007/PL00006190>
- Miller MA, Pfeiffer W, Schwartz T (2010) Creating the CIPRES Science Gateway for inference of large phylogenetic trees. In: 2010 Gateway Computing Environments Workshop (GCE), 1–8. <https://doi.org/10.1109/GCE.2010.5676129>
- Minh BQ, Nguyen MAT, von Haeseler A (2013) Ultrafast approximation for phylogenetic bootstrap. *Molecular Biology and Evolution* 30(5): 1188–1195. <https://doi.org/10.1093/molbev/mst024>
- Nashriq I, Davis HR, Bauer AM, Das I (2022) Three new species of *Cnemaspis* (Sauria: Gekkonidae) from Sarawak, East Malaysia, Borneo. *Zootaxa* 5120(1): 1–29. <https://doi.org/10.11646/zootaxa.5120.1.1>
- R Core Team (2021) R: A language and environment for statistical computing. R Foundation for Statistical Computing, Vienna, Austria. <https://www.R-project.org/>
- Rambaut A, Drummond AJ, Xie D, Baele G, Suchard MA (2018) Posterior summarization in Bayesian phylogenetics using Tracer 1.7. *Systematic Biology* 67(5): 901–904. <https://doi.org/10.1093/sysbio/syy032>
- Riyanto A, Munir M, Martamenggala AIS, Fitriana YS, Hamidy A (2019) Hiding in plain sight on Gunung Muria: a new species and first record of rock gecko (*Cnemaspis* Strauch, 1887; Squamata, Gekkonidae) from Java, Indonesia. *Zootaxa* 4608(1): 155–173. <https://doi.org/10.11646/zootaxa.4608.1.9>

- Ronquist F, Teslenko M, van der Mark P, Ayres DL, Darling A, Höhna S, Larget B, Liu L, Suchard MA, Huelsenbeck JP (2012) MrBayes 3.2: Efficient Bayesian phylogenetic inference and model choice across a large model space. *Systematic Biology* 61(3): 539–542. <https://doi.org/10.1093/sysbio/sys029>
- Rujirawan A, Yodthong S, Ampai N, Termprayoon K, Aksornneam A, Stuart BL, Aowphol A (2022) A new rock gecko in the *Cnemaspis siamensis* group (Reptilia, Gekkonidae) from Kanchanaburi Province, western Thailand. *Zoosystematics and Evolution* 98(2): 345–363. <https://doi.org/10.3897/zse.98.89591>
- Sidisunthorn P, Gardner S, Smart D (2006) Cave of northern Thailand. River Books Co., Ltd, Bangkok, 392 pp.
- Simmons JE (2015) Herpetological collecting and collections management, 3rd edn. Society for the Study of Amphibians and Reptiles Herpetological Circular No. 42. Salt Lake City, UT, 191 pp.
- Smith MA (1925) IV. —Contributions to the herpetology of Borneo. The Sarawak Museum Journal 3(8): 15–34.
- Smith MA (1943) The Fauna of British India, Ceylon and Burma, including the whole of the Indo-Chinese Sub-Region. Reptilia and Amphibia. 3 (Serpentes). Taylor and Francis, London, 583 pp.
- Sumontha M, Kunya K, Dangsri S, Pauwels OSG (2017) *Oligodon sai yok*, a new limestone-dwelling kukri snake (Serpentes: Colubridae) from Kanchanaburi Province, western Thailand. *Zootaxa* 4294(3): 316–328. <https://doi.org/10.11646/zootaxa.4294.3.2>
- Suwannapoom C, Sumontha M, Tunprasert J, Ruangsuwan T, Pawangkhanant P, Korost DV, Poyarkov NA (2018), A striking new genus and species of cave-dwelling frog (Amphibia: Anura: Microhylidae: Asterophryinae) from Thailand. *PeerJ* 6:e4422. <https://doi.org/10.7717/peerj.4422>
- Tamura K, Stecher G, Kumar S (2021) MEGA11: Molecular evolutionary genetics analysis version 11. *Molecular Biology and Evolution* 38(7): 3022–3027. <https://doi.org/10.1093/molbev/msab120>
- Thorpe RS (1975) Quantitative handling of characters useful in snake systematics with particular reference to intraspecific variation in the Ringed Snake *Natrix natrix* (L.). *Biological Journal of the Linnean Society* 7(1): 27–43. <https://doi.org/10.1111/j.1095-8312.1975.tb00732.x>
- Thorpe RS (1983) A review of the numerical methods for recognising and analysing racial differentiation. In: Felsenstein J (Ed.) *Numerical Taxonomy*. NATO ASI Series, Volume 1. Springer, Berlin, Heidelberg, 404–423. https://doi.org/10.1007/978-3-642-69024-2_43
- Trifinopoulos J, Nguyen LT, von Haeseler A, Minh BQ (2016) W-IQ-TREE: a fast online phylogenetic tool for maximum likelihood analysis. *Nucleic Acids Research* 44(W1): W232–W235. <https://doi.org/10.1093/nar/gkw256>
- Turan C (1999) A note on the examination of morphometric differentiation among fish populations: The truss system. *Turkish Journal of Zoology* 23(3): 259–263.
- Uetz P, Freed P, Aguilar R, Reyes F, Kudera J, Hošek J [Eds] (2024) The Reptile Database, <http://www.reptile-database.org>, [accessed 10 September 2024]
- van Beynen PE (2011) Introduction. In: van Beynen PE (Ed.) *Karst management* 2011th edn. Springer, New York, 1–5. https://doi.org/10.1007/978-94-007-1207-2_1
- Wilcox TP, Zwickl DJ, Heath TA, Hillis DM (2002) Phylogenetic relationships of the dwarf boas and a comparison of Bayesian and bootstrap measures of phylogenetic support. *Molecular Phylogenetics and Evolution* 25(2): 361–371. [https://doi.org/10.1016/S1055-7903\(02\)00244-0](https://doi.org/10.1016/S1055-7903(02)00244-0)
- Wood Jr PL, Grismer LL, Aowphol A, Aguilar CA, Cota M, Grismer MS, Murdoch ML, Sites Jr JW (2017) Three new karst-dwelling *Cnemaspis* Strauch, 1887 (Squamata;

Gekkonidae) from Peninsular Thailand and the phylogenetic placement of *C. punctatouuchalis* and *C. vandeventeri*. PeerJ 5: e2884. <https://doi.org/10.7717/peerj.2884>
Yodthong S, Rujirawan A, Stuart BL, Grismer LL, Aksornneam A, Termprayoon K, Ampai N, Aowphol A (2022) A new species in the *Cyrtodactylus oldhami* group (Squamata, Gekkonidae) from Kanchanaburi Province, western Thailand. ZooKeys 1103: 139–169. <https://doi.org/10.3897/zookeys.1103.84672>

Supplementary material 1

Samples used in the molecular analyses, including their locality, voucher number and GenBank accession number

Authors: Attapol Rujirawan, Akrachai Aksornneam, Siriporn Yodthong, Parinya Pawangkhanant, Bryan L. Stuart, Anchalee Aowphol

Data type: xlsx

Explanation note: Voucher abbreviations are the School of Agriculture and Natural Resources, University of Phayao (AUP), Monte L. Bean Life Science Museum at Brigham Young University (BYU), California Academy of Sciences (CAS), the Field Museum of Natural History, Chicago, Illinois, USA (FMNH), La Sierra University Herpetological Collection (LSUHC), Universiti Sains Malaysia Herpetological Collection at the Universiti Sains Malaysia, Penang, Malaysia (USMHC), Zoological Museum of Kasetsart University (ZMKU) and the Zoological Museum of Moscow University (ZMMU).

Copyright notice: This dataset is made available under the Open Database License (<http://opendatacommons.org/licenses/odbl/1.0/>). The Open Database License (ODbL) is a license agreement intended to allow users to freely share, modify, and use this Dataset while maintaining this same freedom for others, provided that the original source and author(s) are credited.

Link: <https://doi.org/10.3897/zookeys.1226.138464.suppl1>

Supplementary material 2

Mean percentages of uncorrected pairwise sequence divergences (*p*-distances)

Authors: Attapol Rujirawan, Akrachai Aksornneam, Siriporn Yodthong, Parinya Pawangkhanant, Bryan L. Stuart, Anchalee Aowphol

Data type: xlsx

Explanation note: Mean (minimum-maximum) percentages of uncorrected pairwise sequence divergences (*p*-distances) of *Cnemaspis* species in the *C. siamensis* group compared to *Cnemaspis enneaporus* sp. nov., based on 1,329 aligned characters of the mitochondrial NADH dehydrogenase subunit 2 gene and flanking tRNAs. Intra-specific *p*-distances are in bold font.

Copyright notice: This dataset is made available under the Open Database License (<http://opendatacommons.org/licenses/odbl/1.0/>). The Open Database License (ODbL) is a license agreement intended to allow users to freely share, modify, and use this Dataset while maintaining this same freedom for others, provided that the original source and author(s) are credited.

Link: <https://doi.org/10.3897/zookeys.1226.138464.suppl2>